Evaluation of the Electroslag Remelting Process in Medical Grade of 316LC Stainless Steel

S. Ahmadi[1)†], *H. Arabi*[2)], *A. Shokuhfar*[3)] *and A. Rezaei*[3)]
1) Institute of Advanced Technologies for Metallic Materials, Tarbiat Modares University, Tehran, Iran
2) Center of Excellence of Advanced Materials and Processing (CEAMP), Department of Metallurgy and Materials Science and Engineering, Iran University of Science & Technology (IUST), Narmak, Tehran, Iran
3) Department of Material Science, Faculty of Mechanical Engineering, K. N. Toosi University of Technology, Tehran, Iran
[Manuscript received May 19, 2008]

This study is focused on the effects of electroslag remelting by prefused slag (CaO, Al_2O_3, and CaF_2) on macrostructure and reduction of inclusions in the medical grade of 316LC (316LVM) stainless steel. Analysis of the obtained results indicated that for production of a uniform ingot structure during electroslag remelting, shape and depth of the molten pool should be carefully controlled. High melting rates led to deeper pool depth and interior radial solidification characteristics, while decrease in the melting rates caused more reduction of nonmetallic inclusions. Large shrinkage cavities formed during the conventional casting process in the primary ingots were found to be the cause of the fluctuation in the melting rate, pool depth and extension of equiaxed crystals zone.

KEY WORDS: Ultra clean steel; Electroslag remelting; Prefused slag; Vertical solidification; Radial solidification

1. Introduction

Medical grade of 316LC stainless steel, *i.e.* 316LVM, low carbon vacuum melted, is widely used for production of the orthopedic implants and proteases. This kind of stainless steel is in the "ultra clean steel" categories, which are manufactured with some special processes such as VIM (vacuum induction melting), VAR (vacuum arc remelting), and ESR (electro slag refining). These processes contribute to reduction of impurity elements (*i.e.* S, O and H) and nonmetallic inclusions, which account for reduction of corrosion resistance[1–3].

During electroslag remelting, casting imperfections, such as shrinkage cavities and macrostructure segregations can be eliminated while microstructure segregations, oxides and sulfide inclusions can be reduced substantially[4–6].

Therefore, processes such as VAR and ESR for producing 316LVM steel are used to prevent the formation of the above mentioned defects or reduce their amounts. In comparison to industrial grade of 316L, the amounts of Cr and Ni in 316LVM have been increased within the range of 17–19 wt pct and 13–15 wt pct, respectively in order to increase its corrosion resistance, but this can cause macrosegregation within its ingot[7–9].

Solidification in electroslaged ingots usually occurs in columnar and equiaxed patterns. Evaluations of these types of structures are accomplished by measuring their secondary arm spacing (SAS). SAS is related to local solidification time parameter (Δt_s) or time needing for reduction of temperature from liquidus to solidus. Relation between the SAS (d) and Δt_s is given as follows[10]:

$$\log d = k_1 + k_2 \log \Delta t_s \quad (1)$$

where k_1 and k_2 are intercept and slope of the curve $\log d$ *vs* $\log \Delta t_s$. Δt_s can be determined by measuring the solidification rate. This rate is the most important parameter for anticipating the macrostructure of electroslaged ingots[11,12].

Some other parameters affecting the electroslag remelting process, such as melting rate, chemical composition of ingot, chemical composition of slag and thermal conductivity pattern have significant influences on the amount of deoxidation of the ingots[13,14]. Elimination of oxide inclusions by chemical reduction and physical flotation reactions can occur in the salt and the melt bath, respectively. Salt bathes in ESR process usually consist of Al_2O_3, CaO and CaF_2 in different amounts[15,16].

In this work, effects of casting rate on the elimination of inclusions and macrostructure of electroslag remelted ingots as well as the effect of double stage deoxidation process of primary electrodes by aluminum and calcium-silicon wires on the cleanness of ingots were studied. Furthermore, for the first time, the effects of casting imperfections (*i.e.* shrinkage cavities) in primary electrodes on the macrostructure of ingots were studied.

2. Experimental

Pure iron, nickel and magnesium with low carbon ferromolybdenum and ferrochromium were used for production of the primary electrodes, as the raw material, in an induction furnace. Alloying process was carried out under argon atmosphere. Some of the electrodes (*i.e.* coded EL101) were deoxidized in two stages using aluminum and calcium-silicon wires. Another electrode (EL102) was deoxidized by pure aluminum wire. The amount of metallic elements, were determined by using spectrometer. Nonmetallic elements such as oxygen, carbon and sulfide were determined by a carbon-sulfide-gas analyzer (CHNOS).

All of the electrodes were subjected to ESR

† Corresponding author. Tel.: +98 261 3505096;
E-mail address: ahmadi.amrc@gmail.com(S. Ahmadi).

Table 1 Melting conditions of the electrodes in ESR process

Ingot code	Electrode code	Weight/kg	Melting time/min	Casting rate/(kg/min)
ES101	EL101	26.12	27.8	0.9
ES102	EL101	25	20	1.2
ES103	EL101	25	33.3	0.7
ES104	EL102	24.5	27	0.9

Table 2 Chemical compositions of the electrodes before ESR process (wt pct)

Electrode code	C	S	P	Ni	Cr	Mo	Mn	O	Fe
EL101	0.027	0.019	0.029	13.58	17.93	2.38	1.59	223×10^{-6}	Rem.
EL102	0.030	0.010	0.013	13.83	17.75	2.45	1.98	54×10^{-6}	Rem.

Table 3 Chemical compositions of the ingots after ESR process (wt pct)

Ingot code	C	S	P	Ni	Cr	Mo	Mn	Al	O	Fe
ES101	0.030	0.005	0.030	13.49	17.83	2.33	1.51	0.01	64×10^{-6}	Rem.
ES102	0.031	0.004	0.031	13.51	17.85	2.37	1.47	0.01	88×10^{-6}	Rem.
ES103	0.030	0.004	0.030	13.55	17.81	2.29	1.49	0.01	48×10^{-6}	Rem.
ES104	0.032	0.002	0.033	13.82	17.72	2.42	1.77	0.05	15×10^{-6}	Rem.

process in a furnace using CaO, Al_2O_3, CaF_2 slag, each having 1/3 of the total weight percent of the slag. Pre-fused slag was heated to about 800°C for eliminating the moisture before ESR process. EL101 electrodes were melted in three different melting rates and the products were recoded as ES101, ES102, and ES103. EL102 electrode was recoded as ES104 after ESR process. Details of melting conditions of the electrodes for production of ingots are given in Table 1.

Morphologies and compositions of the inclusions were studied using scanning electron microscopy (SEM, Cam Scan MV2300) equipped with EDS (energy dispersive X-ray spectrometer). In addition, sizes and distribution of inclusions were determined with LEICA MW image analyzer program.

3. Results and Discussion

3.1 Macrostructure of ingots

The chemical compositions of the electrodes before and after ESR are given in Tables 2 and 3. The results show that, using the slag with equal amounts of CaO, Al_2O_3 and CaF_2 (*i.e.* each having 1/3 of the total weight of the slag) led to reduction of oxygen by 60% and sulfur by 70%. Reduction of sulfur during ESR can occur by two mechanisms: reaction between slag (especially CaF_2) and sulfuric inclusions, and reaction of sulfur with oxygen of the atmosphere. These reactions can be presented as follows:

$$[S] + (O^{2-}) \rightarrow (S^{2-}) + [O] \quad (2)$$

$$(S^{2-}) + 3/2(O^2)_g \rightarrow (SO_2)_g + (O^{2-}) \quad (3)$$

The amount of alloying elements, *e.g.* Ni, Cr, Mo and Mn are almost constant after ESR process (see Tables 2 and 3). Macrostructures of the ingots are shown in Figs. 1–4.

These Figures show that the overall shape of grains in ES101, ES102 and ES103 ingots are columnar whereas ES104 ingot has a near globular grains zone structure at center. Electrode of the ES104 ingot constituted of four primary electrodes, which were welded together. These primary electrodes had some

Fig. 1 Macrostructure of ES101 ingot (outer diameter, ϕ=14 cm)

Fig. 2 Macrostructure of ES102 ingot (outer diameter, ϕ=14 cm)

cavities as imperfections developed during the conventional casting. Therefore, the presence of these

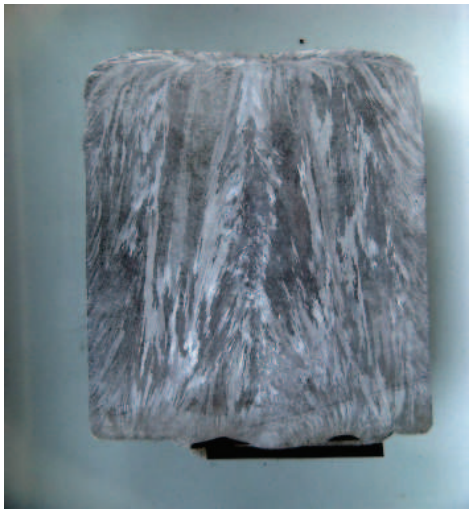

Fig. 3 Macrostructure of ES103 ingot (outer diameter, ϕ=14 cm)

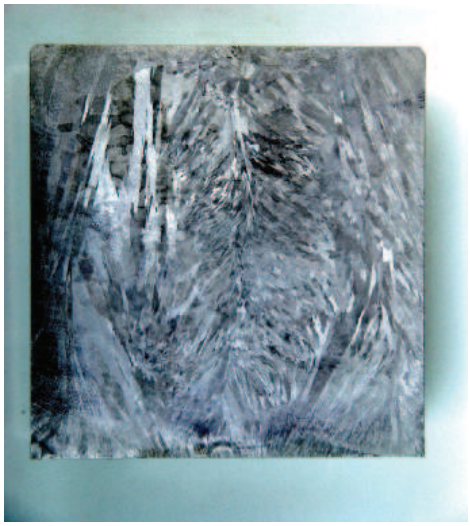

Fig. 4 Macrostructure of ES104 ingot (outer diameter, ϕ=14 cm)

cavities may have caused some fluctuation in the current and voltage used during ESR process; this can be the main reason for development of some globular grain zone within the columnar structure of ES104 ingot. In fact, fluctuation in current and voltage can cause fluctuation in melting rate within the melt bath, which is the most important parameter to change the nature of grains pattern from vertical to radial and *vice versa*.

The melting conditions presented in Table 1 and the typical macrostructures in Figs.1–3 show that by increasing the melting rate, grains grow in the radial direction (Fig. 2) while by decreasing the melting rate, grains grow in the vertical direction (Fig. 3). The variation in grain pattern can be related to melting rate and the depth of melt in the bath.

Relation between the thermal conductivity coefficients of solid (K_s) and liquid (K_L), gradients of the solidus (G_s) and liquidus (G_L) isotherms, enthalpy of melting (ΔH_f) and density (ρ) has been presented in literature [17]:

$$K_s G_s - K_L G_L = \rho \cdot \Delta H_f \cdot U_n \tag{4}$$

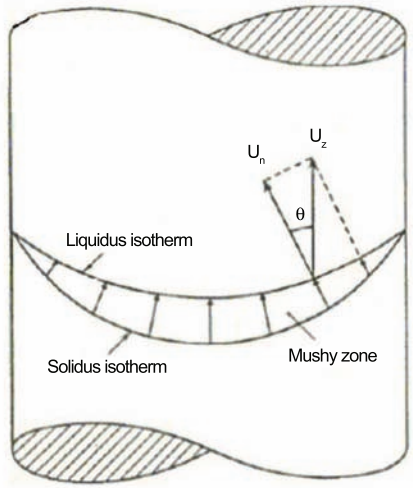

Fig. 5 Solidus and liquidus isotherms, mushy zone and direction of the U_n[17]

where U_n is melting rate, which is a function of casting rate (U_z) according to Anable *et al.*[17] and can be calculated by the following relationship:

$$U_n = U_z \cdot \cos\theta \tag{5}$$

Schematic relation between solidus and liquidus isotherms, mushy zone and direction of the U_n proposed by Anable *et al.*[17] is shown in Fig. 5. For metals, in general K_L is equal to $0.5K_s$. Substituting K_L=$0.5K_s$ in Eqs. (4) and (5), G_s as a function of U_n can be calculated.

$$G_s - 0.5G_L = U\left(\frac{\rho \cdot \Delta H_f \cdot \cos\theta}{K_s}\right) \tag{6}$$

Depth and shape of the melt bath are determined by the differences between the gradient of the solidus and liquidus isotherms. Furthermore, these parameters determine the size and shape of the mushy zone in ESR process[17]. In fact, by increasing the casting rate (U_z) and melting rate (U_n), the difference between the gradient of the solidus and liquidus isotherms and depth of melt bath (G_s−G_L) increases. Hence, grains grow in radial direction instead of vertical direction. Figures. 1–4 and Table 2 confirm these results.

3.2 Elimination of inclusions

In Tables 4 and 5, some characteristics of the inclusions in electrodes and ingots are given. When primary electrodes deoxidized by aluminum (EL102) or by calcium-silicon wire (EL101), inclusions were formed by the following reactions:

$$2[\mathrm{Al}] + 3[\mathrm{O}] \rightarrow \mathrm{Al_2O_{3(s)}}$$

$$\Delta G^0_{1873\ \mathrm{K}} = -1075103.6(\mathrm{J}) \tag{7}$$

$$3[\mathrm{Ca}] + (\mathrm{Al_2O_3}) \rightarrow 3(\mathrm{CaO}) + 2[\mathrm{Al}]$$

$$\Delta G^0_{1873\ \mathrm{K}} = -213573(\mathrm{J}) \tag{8}$$

$$x\mathrm{CaO} + y\mathrm{Al_2O_3} \rightarrow (\mathrm{CaO})_x(\mathrm{Al_2O_3})_y \tag{9}$$

The characteristics of inclusions in the cast electrodes and electroslag remelted ingots presented in Tables 4 and 5 shows that one or two stage deoxidation process has significant effects on the size and number of the

Table 4 Dimensions of inclusions within the primary electrodes

Electrode code	No. of inclusions per unit area (mm^2)	Maximum diameter/μm	Minimum diameter/μm	Average diameter/μm	Total surface of inclusions/ surface of specimen
EL101	136	47	6	16	0.25%
EL102	112	22	4	10	0.32%

Table 5 Dimensions of inclusions within the ingots (after ESR process)

Ingot code	No. of inclusions per unit area (mm^2)	Maximum diameter/μm	Minimum diameter/μm	Average diameter/μm	Total surface of inclusions/ surface of specimen
ES101	104	36	5	13	0.15%
ES102	114	41	7	14	0.17%
ES103	84	35	4	14	0.13%
ES104	262	18	2	5	0.30%

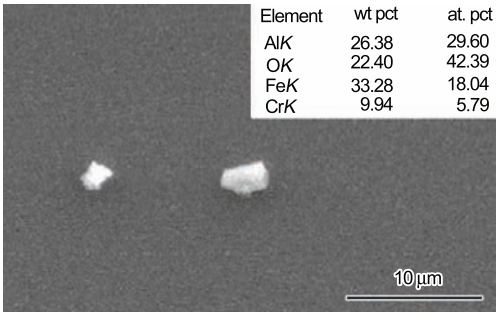

Fig. 6 Alumina inclusion in ES104 ingot

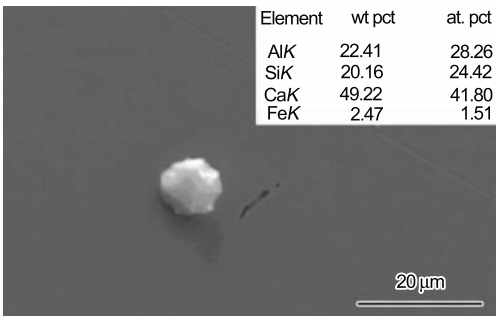

Fig. 7 Alumina-calcia complex inclusion in ES101 ingot

inclusions. Deoxidation of electrodes before ESR by aluminum was seemed to be responsible for formation of smaller inclusions whereas the number of inclusions in these ingots was higher than that of other ones.

Elimination of inclusions in ESR is affected by the rotative motion of the melt under the slag bath. Therefore, the important mechanisms for reducing the inclusions in the melt and slag baths consist of flotation of inclusions on the melt bath, adherence of inclusions to the slag and chemical reaction between the slag and inclusions. These sequences were more effective for reduction of alumina-calcia inclusions than the alumina inclusions in the present study. This is due to the fact that alumina inclusions have higher melting point, smaller size and more stability than alumina-calcia inclusions; as a result, elimination of this kind of inclusions in the slag bath by chemical reactions is almost impossible.

Complex inclusions, such as alumina-calcia have lower melting point than the alumina inclusions and can be floated easily on the melt bath by contact and adherence. Therefore, cleanness of the electroslag remelted ingots having complex inclusions (*e.g.* alumina-calcia) is expected to be higher than the other ingots, which deoxidized in one stag by aluminum. Typical alumina and alumina-calcia inclusions are shown in Figs. 6 and 7.

Another parameter affecting the elimination of inclusions in the samples subjected to ESR was the melting rate. The melting parameters presented in Table 1 show that in ES101, ES102 and ES103 ingots, with the same deoxidation process, decrease in casting rate contributes to more cleanness of 316LVM steel ingots after ESR. The number of inclusions and the amount of oxygen in ES103 ingot, which was remelted by the lowest casting rate (0.7 kg/min), were less than those of the other ingots. Increasing the casting rate is responsible for passing the melt drops through out the slag bath quickly and therefore resulted in decrease in the elimination of inclusions.

4. Conclusions

(1) Using $CaO+Al_2O_3+CaF_2$ slag in the electroslag remelting process of 316LVM stainless steel, caused reduction of oxygen and sulfur about 60%.

(2) Increase in the casting rate changed the characteristic of solidification from vertical to radial and decreased the elimination of nonmetallic inclusions.

(3) Presence of the shrinkage cavities in the primary electrodes caused fluctuation in the melt pool, which resulted in formation of heterogeneous macrostructure in the electroslag remelted ingots.

(4) Use of double stage deoxidation process for elimination of oxides and inclusions (*i.e.* using aluminum and calcium- silicon wires) during ESR was more effective than the use of single deoxidation process by aluminum or calcium-silicon wire.

REFERENCES

[1] S.V. Bhat: *Biomaterials,* Alpha Science International Ltd., New Delhi, India, 2002, 13.

[2] J.R. Davic: *Handbook of Materials for Medical Devices,* ASM Int., New York, 2003, 51.

[3] F.H. Silver: *Biomaterials Medical Devices and Tissue Engineering,* Chapman & Hall, New Jersey, 1994, 4.

[4] G. Hoyle: *Electroslag Remelting Process,* Science Publisher Company, 1983, 5.

[5] H.J. Mueller-Aue, D. Hengerer and W. Holzgruber: *Trans. Indian Inst. Met.,* 1980, **33**(2), 85.

[6] A.C. Kell: Metals Hand Book, Elsevier Publication, 1995, 401.
[7] A.F.V. Recum: *Handbook of Biomaterials Evaluation,* Taylor and Franeis, London, 1999, 13.
[8] G.L. Winters and M.J. Nutt: *Stainless Steel for Medical and Surgical Applications,* ASM Int., New York, 2003, 3.
[9] J.A. Disegi and L. Eschbach: *Injury,* 2000, **31**(Suppl. 4), D2.
[10] P.O. Mellberg and H. Sandberg: *Scand. J. Metall.,* 1973, **2**, 83.
[11] A. Mitchell and R.M. Smailer: *Int. Metal. Rev.,* 1979, **5-6**, 231.
[12] L.A. Bertram P.R. Schunk, S.N. Kempka, F. Spadafora and K. Minisandram: *JOM,* 1998, **50**(3), 18.
[13] L. Zhenobang: *Problemy Spetsial'noi Elektrometallurgii,* 1998, **5**, 30.
[14] W.E. Dukworth and G. Hoyle: *Brit. Iron Steel Res.,* 1989, **3**, 26.
[15] A.S. Rao, V.V.S. Prasad, R.G. Baligidad, V.R. Rao and D.S. Sarmar: *Trans. Indian Inst. Met.,* 1999, **52**(2-3), 139.
[16] G. Balachandran, M.L. Bhatia, N.B. Ballal and P. Krishna Rao: *ISIJ Int.,* 2000, **40**, 478.
[17] W.E. Anable, R.H. Nafziger and D.C. Robinson: *JOM,* 1973, **25**(11), 55.